https://doi.org/10.5194/tc-2021-21
Preprint. Discussion started: 12 March 2021

The Cryosphere Discussions

Accelerated decline of Svalbard coasts fast ice as a result of climate change

Jacek A. Urbański[1], Dagmara Litwicka[1]

[1]GIScience Laboratory, Institute of Oceanography, University of Gdansk, Gdynia, 81-378, Poland

Correspondence to: Jacek A. Urbański (jacek.urbanski@ug.edu.pl)

Abstract. In the Arctic, it is the Svalbard Archipelago that has experienced some of the most severe temperature increases in the last three decades. The temperature rise has accelerated de-icing along the archipelago's coasts, bringing changes to the local environment. As the fast ice distribution along Svalbard coasts before 2000 is mainly unknown, we use *in situ* observation data of the ice extent for the period of 2005-2018 to create a new geographic random forest model in order to predict daily ice extents using freezing and thawing degree days and time of ice season. This allows one to reconstruct the ice extent in the past and predict it in the near future from standard meteorological data with an accuracy of 0.95. The mean, at least two-month ice extent of fast sea ice along Svalbard coasts was about 12,000 km^2 between 1973 and 2000. In 2005-2018, however, the same ice extent declined to 8,000 km^2. Comparison of the periods 2005-2018 and 2014-2019 shows the accelerating decline of fast ice: the two-month fast ice extent is now only 6,000 km^2. A further increase in mean winter air temperatures by two degrees will result in a two-month fast ice extent of 2,000 km^2.

1. Introduction.

The Svalbard Archipelago is the largest land area in the European part of the Arctic. Its location is strongly influenced by the West Spitsbergen Current and the semi-continuous weather front between the cold masses of Arctic air and the warmer air of the polar cell. As a result, climate changes there are magnified: indeed, the Arctic has experienced one of the biggest increases in temperature in the present century (Isaksen et al., 2016). During the last 40-50 years, the temperature has risen by 4-5 °C (Hanssen-Bauer et al., 2019). Meteorological observations made since the beginning of the 20th century show that the air temperature has always fluctuated in this region. But whereas between the 1960s and the early 1990s winter air temperatures were only slightly higher than at the beginning of the 20th century, by the beginning of the 21st century, temperature rises were starting to accelerate and are continuing to do so (Nordli et al., 2014). Figure 1 illustrates the changes in the mean annual and the mean temperature in the winter half of the year, when fast ice mainly occurs. Current forecasts envisage a mean annual temperature rise in this region of at least 1 °C per decade until the mid-21st century (Hanssen-Bauer et al., 2019). Because of the low air temperature and the highly indented coastline, the coastal waters of Svalbard are every year covered by fast ice, i.e. ice that holds fast to the coastline or the sea bottom. This usually accumulates in fjords, between islands, and in shallow inshore waters. In the Arctic, fast ice is biologically important as a breeding and moulting site for seals, mainly ringed seals (*Pusa*

https://doi.org/10.5194/tc-2021-21
Preprint. Discussion started: 12 March 2021

The Cryosphere Discussions
Open Access
EGU

hispida), the principal prey of polar bears (*Ursus maritimus*) (Krafft et al., 2006; Smith and Lydersen, 1991). Moreover, for as long as it persists, fast ice protects coastal areas from erosion by wave action.

The precision monitoring of local sea ice conditions in the fjords and coastal waters of Svalbard began just under 20 years ago (Hanssen-Bauer et al., 2019) using new technology of high and medium resolution satellite images, mainly from C-band Synthetic Aperture Radar (SAR) sensors, and GIS-based automatic or semi-automatic systems for sea ice classification (Zakhvatkina et al., 2019). Previously, ice conditions used to be assessed mainly from *in situ* observations made as part of various ice-monitoring programmes; they revealed a general trend towards a smaller ice extent and a decrease in ice thickness compared to a few decades earlier (Gerland et al., 2008; Hanssen-Bauer et al., 2019; Zhuravskiy et al., 2012). From 1974 to 1988, analyses of the total number of days with fast ice before 1st April (the ring seal pupping date) were based on satellite data: a strong interannual variability ranging from 0 to 155 days was detected in the fjords of northern Spitsbergen (the largest island of Svalbard) and from 38 to 107 days on the western coast (Smith and Lydersen, 1991). Most of the ice monitoring projects were carried out on the west coasts of Svalbard. Between 2000-2014, analysis of the temporal changes in the ice cover in Isfjord and Hornsund using SAR and optical images revealed a significant decrease in the extent of fast ice in both fjords in that period (Muckenhuber et al., 2016). Systematic observations in Kongsfjord since 2003 initially detected, as in the 1970s and 1980s, substantial interannual variability in fast ice extent with intervals of 2-3 years or more. More recent observations have indicated that the ice extent is less in most years and that the fast ice season is becoming shorter (Gerland and Hall, 2006; Gerland and Renner, 2007; Alexey K. Pavlov, 2019). There has been less fast ice -off the northern coasts of Svalbard, although occasional observations have shown that the fast ice cover can last from November until July (Wang et al., 2013). Since 2005, ice charts of the Svalbard area have been produced almost daily (Monday-Friday) by the Norwegian Ice Service. As the charts are based on current data, it has been possible to gradually improve their accuracy.

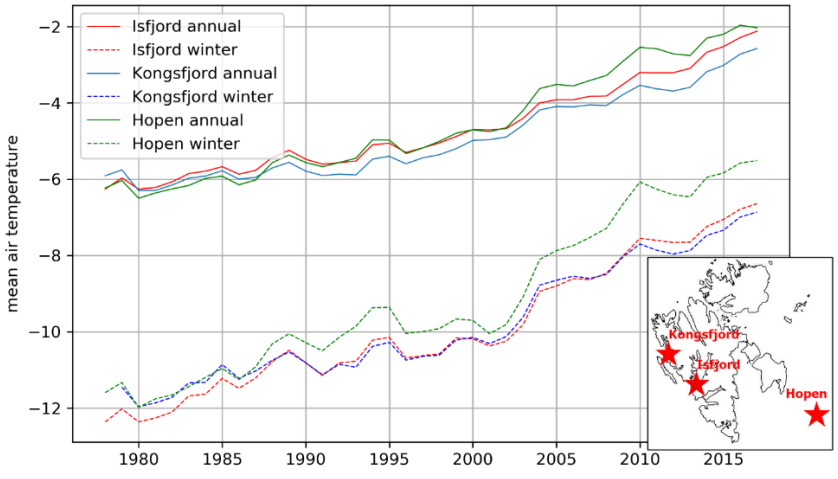

https://doi.org/10.5194/tc-2021-21
Preprint. Discussion started: 12 March 2021

Figure 1: Air temperature changes at three meteorological stations in the Svalbard Archipelago (1975 – 2018). The solid lines show the annual mean, and the dashed lines the winter (December – May) mean. Eight-year smoothing using a rolling yearly mean was used. Isfjord – Barentsburg meteorological station (78.1, 14.3), Kongsfjord – Ny Alesund meteorological station (76.5, 25.0667), Hopen meteorological station (78.923, 11.9331).

The duration of fast ice cover around Svalbard has become perceptibly shorter in the last ten years (Alexey K. Pavlov, 2019), so a knowledge of the mean temporal distribution of that fast ice is essential to many projects. Unfortunately, this distribution in the last quarter of the 20th century is unknown. If we had this knowledge, we would be able to compare the two distributions so as to obtain a picture of the changes in the coastal environment due to the increase in air temperature (Nordli et al., 2014). Hence, the primary aim of the present research was to characterize the spatial distribution of the mean temporal difference in the presence of fast ice between 1975-2000 and 2014-2019 at the archipelago scale and the fjord scale. The second aim was to quantify the changes in the fast ice surface area in different time periods, i.e. in the two periods mentioned above, and in the near future, assuming the forecast increase in temperature.

2. Datasets of in situ observations.

Meteorological data for 1973-2019 were acquired from the Global Historical Climate Network (GHCN) for the Hopen, Barentsburg and Ny Alesund stations as daily summaries in text file format (Menne et al., 2012). Scans of operational ice charts produced by the Norwegian Ice Service in 2005-2018 for the Svalbard Archipelago were downloaded from the archive dataset of the Norwegian Meteorological Institute. The 900 map scans, created using different methods, were automatically downloaded in raster formats of .gif, .jpg. and png using Python script. In addition, 55 Landsat satellite images showing Isfjord covered by ice in 1973-1998 were acquired (by courtesy of the U.S. Geological Survey). The GIS vector and raster layers with a georeferenced coastline and land-water mask of the Svalbard Archipelago were obtained from GIS Centre, University of Gdańsk.

3. Data pre-processing.

The meteorological data were pre-processed using the Python libraries pandas and numpy and visualized with matplotlib and seaborn. These data contained fields with incomplete values of mean, maximum and minimum daily temperature. The workflow of the pre-processing of these data involved the following steps. Separate data sets for each station were created starting from 1 September 1973. Missing maximum and minimum temperatures were filled in by linear interpolation. Then linear regression modelling was used to estimate the average daily temperature (TAVG) from minimum and maximum values. The regression equation was used to fill gaps in the TAVG in each data set. These sets were used to create Figure 1.

https://doi.org/10.5194/tc-2021-21
Preprint. Discussion started: 12 March 2021

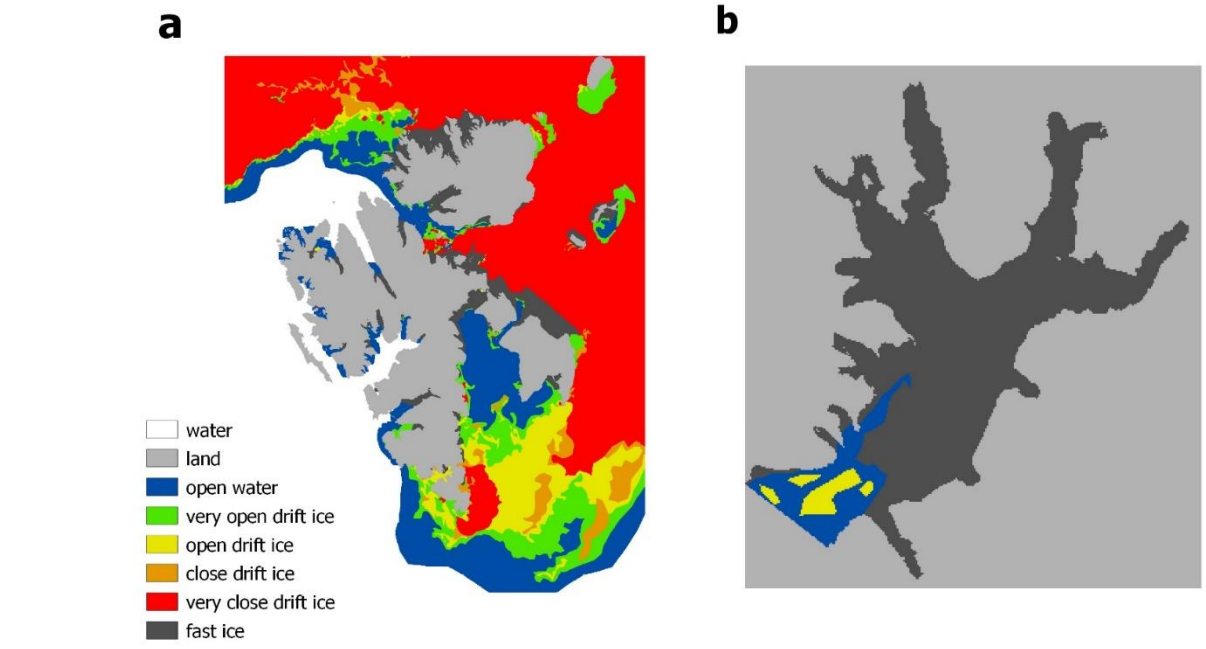

Figure 2: Raster maps of the Svalbard Archipelago (a) and Isfjord(b). The rasters have a spatial resolution of 300 m and contain integer values for classes (Water - 0, Land - 1, Open water - 2, Very Open Drift Ice - 3, Open Drift Ice - 4, Close Drift Ice - 5, Very Close Drift Ice - 6, Fast Ice - 7).

The next step was to calculate for each day the freezing degree days (FDD) and thawing degrees days (TDD) at Isfjord employing Stefan's Law (Lepparanta, 1993):

$$FDD = \int_0^t [T_f - T_0(t)]\, dt \quad for\ T_0 < T_f \qquad (1)$$

$$TDD = \int_0^t [T_0(t) - T_f]\, dt \quad for\ T_0 > T_f \qquad (2)$$

where t is time, T_f is the freezing temperature (0 ºC according to the Polar Science Centre) and $T_0(t)$ is the average daily temperature. The formulas usually use one day as the unit of time. The FDD is also called the sum of negative degree days and is used to simplify the formula for estimating ice thickness (Lepparanta, 1993): it sums the below-zero temperatures for each successive day. TDD is similar but for temperatures above 0 ºC. It was assumed that the ice season starts on 1st September and lasts for 300 days, until the end of June. The definition of the ice season allows the number of ice seasons (ICESN) and the day number of a particular ice season (ICESD) to be assigned to each day. As a result, a text file was created for 13 794 days (1.09.1973 – 27.06.2019) with columns: Time, Year, Month, Day, TAVG, FDD, TDD, ICESD, ICESN. The file *METEO_ISFJORD.CSV* is included in the SUPPLEMENT.

In the second step, the scanned ice cover maps were manually or automatically digitized to two time series of rasters with the following classes: 0 – water, 1 – land, 2 – open water, 3 – very open drift ice, 4 – open drift ice, 5 – close drift ice, 6 – very close drift ice, 7 – fast ice. The spatial resolution of the rasters was 300 m. The satellite images were manually digitized on-screen using the same classification and converted to rasters. Two time series of rasters were prepared: one for the Svalbard

https://doi.org/10.5194/tc-2021-21
Preprint. Discussion started: 12 March 2021

Archipelago (806 rasters, 1533 x 1957 pixels) and the other for Isfjord (956 rasters, 290 x 322 pixels). These maps are exemplified in Figure 2.

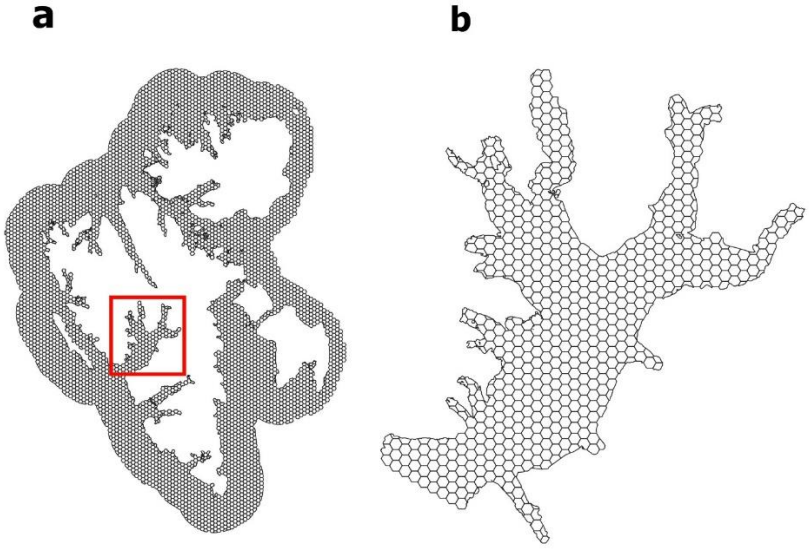

Figure 3: Vector hexagon nets for the Svalbard Archipelago (a) with 4782 cells and Isfjord (b) with 669 cells. The red rectangle shows the location of Isfjord.

The georeferenced rasters were saved in GeoTiff format. Two hexagon nets, both with a unique ID and respective cell areas of 16 km^2 and 4 km^2, were created for the Svalbard Archipelago and Isfjord (see Figure B2). The information from the raster data series was combined with that contained in the daily text files with meteorological data and calculated FDD and TDD values. Two new text files were created. For each raster of the ice cover, a new row of data was created containing all fields from METEO_ISFJORD for a particular day, supplemented with columns for each hexagon cell with values 1 (ice presence) or 0 (ice absence). A field with the sum of ice-covered cells was also added. The file for the Svalbard Archipelago (METEO_ICE_SVALBARD.CSV) contains 793 rows describing the meteorological and ice situation for a particular day in 4791 columns (Time, Year, Month, Day, TAVG, FDD, TDD, ICESD, ICESN, ICESUM, R1…R4782). The columns R1…R4782 contain ice cover data for each cell, and the ICESUM field sums them up. The file for Isfjord (METEO_ICE_ISFJORD.CSV) has a similar format and contains 669 columns with ice cover values (R1…R669). Comparison of the raster maps used in this project (observed ICESUM) with published accurate data for Isfjord (Lutz et al., 2018) confirms their reliability. These files have a tidy structure, i.e. the standard data structure for machine learning libraries. Each variable creates a column and each observation creates a row. Both files are included in the SUPPLEMENT.

4. Machine learning modeling.

The Random Forest (RF) regression and classification model was used to predict ice cover as percentages (ICESUM) and to classify the hexagon net cells for two classes (ice/ no ice) on any day using FDD, TDD and ICSN as features. The Random Forest model, introduced by Breiman (Breiman, 2001), has been used in many geophysical and environmental applications

https://doi.org/10.5194/tc-2021-21
Preprint. Discussion started: 12 March 2021

(Lutz et al., 2018; Mutanga et al., 2012; Rodriguez-Galiano et al., 2014, 2015). In this method, random decision trees are created by bootstrapping data in which the samples are drawn with replacement. Then the majority vote or average predictions of all trees is used to generate results. The main advantages of the RF model are that overfitting can be reduced by averaging several trees, and that no statistical assumptions regarding normal distribution and data linearity are necessary. The model also allows one to measure the relative importance of each feature for the prediction. It is easy to apply, and the few default hyperparameters usually give good results. One of the model's shortcomings, however, is that extrapolation beyond the range of values in the training set is not possible. The typical workflow is to use a training set (containing the dependent variable and the independent variables) to learn the RF model, and then to validate the results using a test data set. One can also validate the results using Out of Bag (OOB) error estimation. We performed the RF modelling using the Python Scikit-learn package (Pedregosa et al., 2011). The first step was to build the RF regression model in order to predict the percentage ice cover in Isfjord (ICESUM) using FDD, TDD and ICESD. The aim was to evaluate the importance of particular features and the overall accuracy of the ice cover modelling. Two measures were applied: the feature importance, implemented in Scikit-learn, which yielded results of 67% (FDD), 18% (ICESD) and 15% (TDD), and the permutation importance, implemented in the eli5 library, with results of 75% (FDD), 21% (ICESD) and 5% (TDD). The accuracy was evaluated using the RMS error: the mean RMS was 0.06 (range 0.052 – 0.074) for 50 random test data sets, each containing 30% of the original data (for the range of ice cover 0-1). These results of ICESUM predictions for Isfjord were regarded as satisfactory. The results of this model for three periods of time are shown in Figure 4.

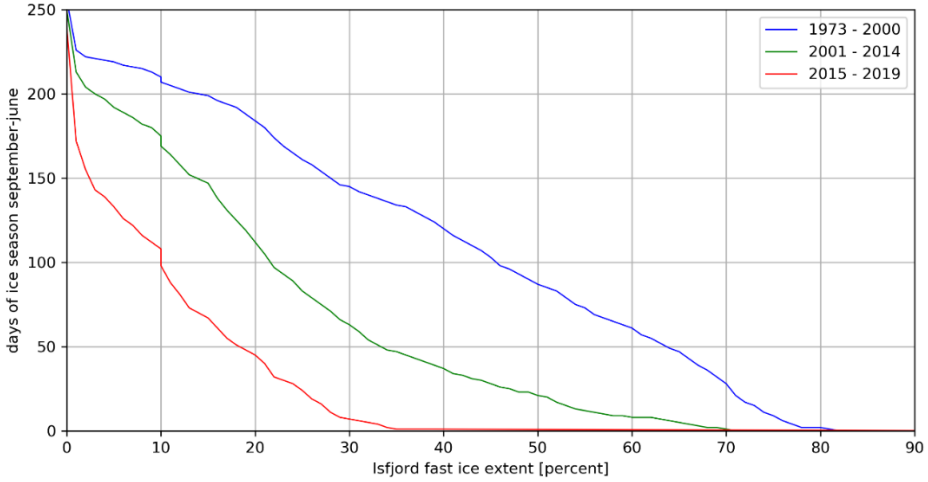

Figure 4: The duration and extent of fast ice cover in Isfjord over three periods of time.

On the basis of these results, the distributed Random Forest classification model was applied to the hexagon nets for the Svalbard Archipelago and Isfjord. Separate models were created for each cell and used to forecast the presence or absence of ice for different time series. This can be summarized by the percentage ice cover in a particular cell in time , which is saved

https://doi.org/10.5194/tc-2021-21
Preprint. Discussion started: 12 March 2021

with the cell's ID to the output file. As each model generates information on the errors arising when using the test data set, these errors can also be saved. The data from this file can be added as a new field to the attribute table of the vector layer of the net to the spatial mapping of ice distribution. The results of the modelling and observations are summarised as vector layers in GeoRF_ICE_MODELS [].zip files containing the Geo File Database and Geo Package formats. The models are built iteratively and the whole process, which we have called Geo Random Forest, is presented in Figure 5.

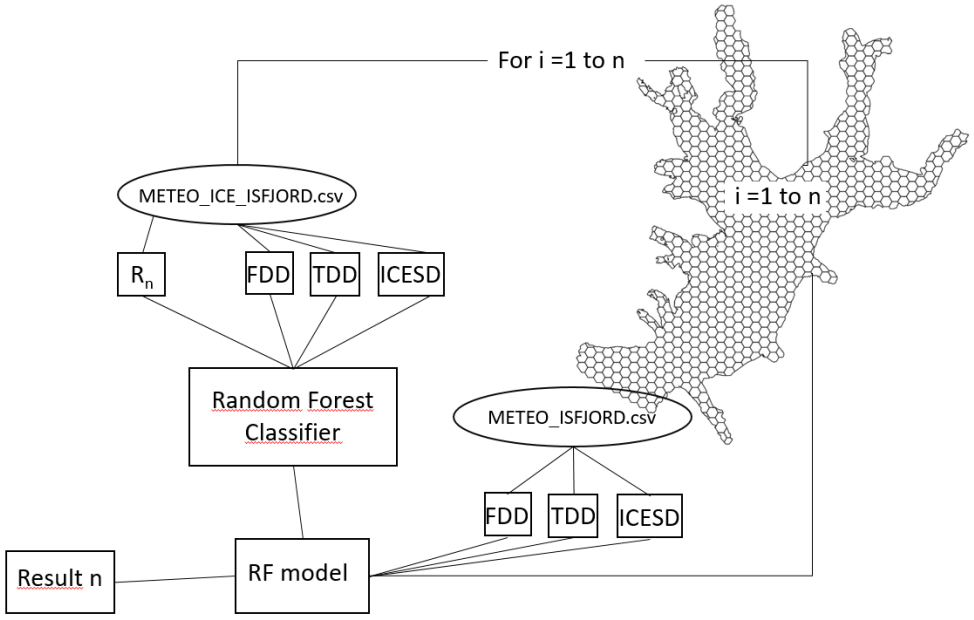

Figure 5: The Geo Random Forest classification model. A separate model is created for each hexagon of the net. This model is used to predict the ice cover for each day of the defined period. The ice cover statistics for this period are saved in the consecutive rows of the output file (Result n).

Modelling local variables in a complex environment using a simplified set of features, which is effective for these variables averaged in space, requires taking local peculiarities into consideration. Local ice cover depends, among other things, on the water depth, wave action, water circulation and local microclimate. In the machine learning process, all these features are irrelevant if the dependent variable (target) represents just a single location. The model uses only basic features from one location, which correlates well in space, but gives a prediction only for that particular location. Figure 6 illustrates the results of error evaluation for the Svalbard Archipelago model as a histogram of errors, calculated for each cell using an independent validation set containing 20% of the original values. The model is created on the assumption that for any net cell, the formation and duration of the ice are determined by the same temporal processes over time. This is probably true for large FDD values, where the difference in external environmental conditions over different periods may not be important. However, their role in young ice cover (less than one month) may be much bigger. In Figure 5 these processes probably increase errors to 20 – 30%. As a result, the errors of predictions for a temperature increase of 2 or 4 °C may be as high as 50%; this, however, does not alter the anticipated trend of dramatic de-icing in this area in the near future.

https://doi.org/10.5194/tc-2021-21
Preprint. Discussion started: 12 March 2021

The Cryosphere Discussions
Open Access
EGU

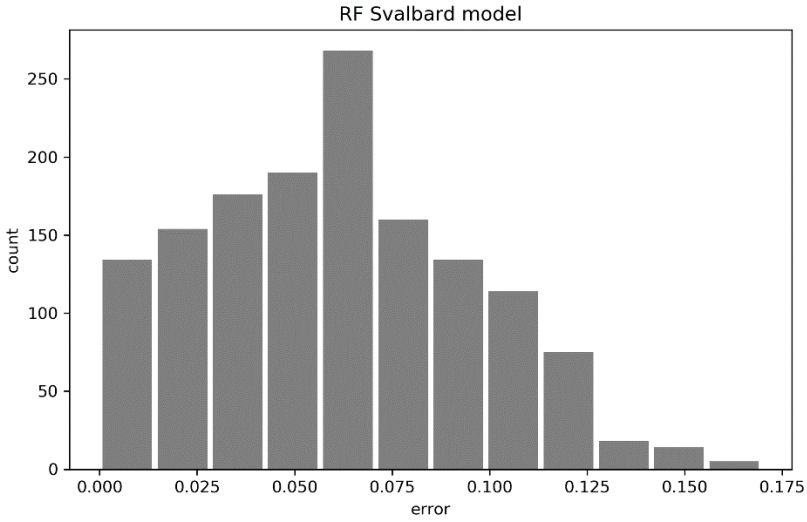

Figure 6: The histogram of model errors (rate of false predictions in the test set) from independent models for all hexagons of the Svalbard net.

5. Discussion.

The AI geographic Random Forest (GeoRF) method was used in this work: it disaggregates the classic method of machine learning (Random Forest) into geographic space in the form of local sub-models. It is an alternative solution to the Geographically Weighted Random Forest (Georganos et al., 2019). Using raster maps of the daily fast ice distribution from 1975 to 2018 and the daily mean temperature, GeoRF sub-models were built to predict the local presence or absence of fast ice as a function of three variables – Freezing Degree Days (FDD), Thawing Degree Days (TDD) and day number of the ice season – which can be calculated from standard meteorological data containing the mean daily air temperature. Comparison of the raster maps used in this project (ice charts produced by the Norwegian Ice Service) with accurate data for Isfjord (Gerland et al., 2008) shows their reliability to be satisfactory. 669 sub-models organized in a 4 km^2 hexagon net for Isfjord and 4782 sub-models in a 16 km^2 net for the whole Svalbard Archipelago were used. The mean accuracy of the GeoRF sub-models was $R^2 = 0.95$ (from 0.84 to 1). The model allows one to predict the presence of fast ice in a hexagon on the basis of mean daily air temperature, which has been measured on Svalbard since the beginning of the 20th century.

https://doi.org/10.5194/tc-2021-21
Preprint. Discussion started: 12 March 2021

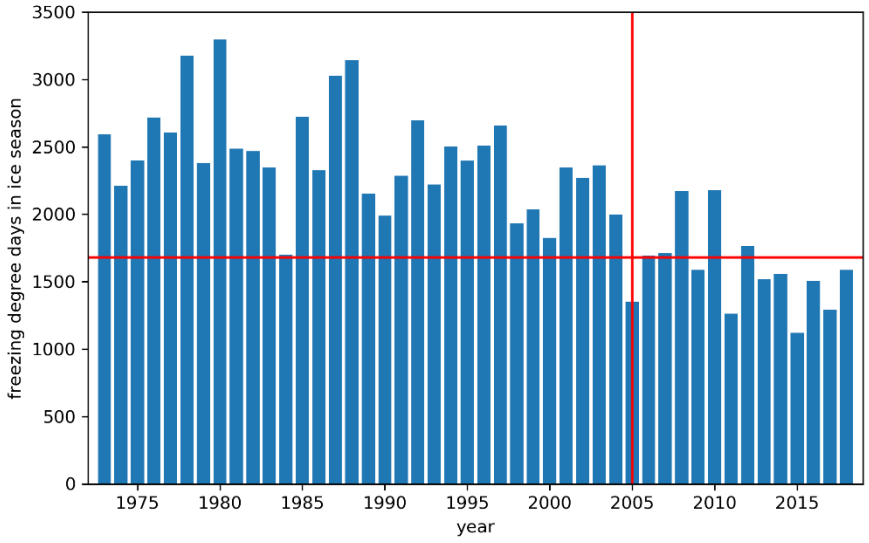

Figure 7: Freezing degree days (FDD) in ice seasons for Isfjord (assigned to the year when the ice season starts) from 1973/74 to 2018/19. The vertical red line indicates the year 2005 as the start of warmer winters, and the horizontal line shows the minimum FDD since 2005.

Owing to its cumulative nature, FDD is the simplest parameter that correlates well with fast ice thickness and its duration. As an ice season straddles two consecutive years, starting in autumn and ending in early summer, all statistics should apply to an ice season rather than a year. Figure 7 shows cumulative FDD for each ice season from 1973/1974 to 2018/2019, the values being assigned to the year when the ice season starts. The results confirm the observed shortening of the fast ice season from 2005/2006 onwards (Alexey K. Pavlov, 2019). Until then, FDD had oscillated with a frequency of a few years, with maximum values exhibiting a decreasing trend. FDD in most ice seasons at that time varied from 2000 to 2500 ºC day. But after 2005/2006, FDD was significantly higher than the minimum in 1973-2005 (32 seasons) in only two of the subsequent 13 seasons. On the other hand, FDD was lower than the minimum (from 1000 to 1500 ºC day) in 9 seasons. Interannual variability still occurs, but the evidently decreasing trend in FDD now applies to both mean and minimum values. Because of the relatively small number of observations, the above analysis is entirely speculative, but it does reflect the general tendencies confirming earlier results (Gerland and Hall, 2006; Gerland and Renner, 2007; Alexey K. Pavlov, 2019).

https://doi.org/10.5194/tc-2021-21
Preprint. Discussion started: 12 March 2021

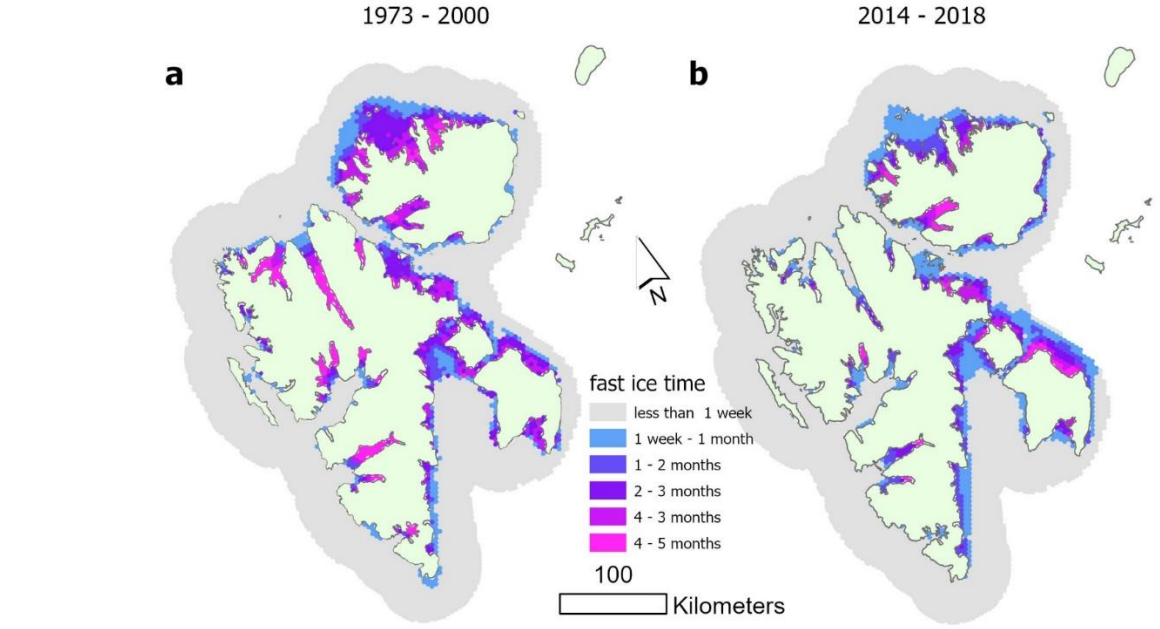

Figure 8: Mean distribution of the fast ice extent (time scale) during the ice seasons in 1973-2000 (a) and 2014-2018 (b). The maps show how long the fast ice lasted in both periods. Map (a) was created using a geographically weighted random forest model, map (b) using observational data.

Figure 8 shows maps of the distribution and duration of fast ice around Svalbard coasts for two periods. The map for 2014-2018 was produced using observational data, whereas the map for 1973-2000 is the result of modelling. Between 1973-2000, at least half of the surface area of the fjords in west Spitsbergen was covered by fast ice for 4 to 5 months, while the fjords in north Spitsbergen were completely covered by fast ice for the same length of time. The north-west Spitsbergen coasts had fast ice cover for 2-3 months. The east coast, where there are no fjords, was covered by fast ice mainly in the bays. Between 2014-2018 the distribution and duration of fast ice cover changed dramatically; in the fjords of west Spitsbergen, fast ice persisted for 4 months only at their heads, whereas those in north Spitsbergen were covered by fast ice for less than half of their lengths, usually for 2 months and only locally for 3 months.

Figure 9 summarizes the changes in the periods under scrutiny for the observed and modelled areas. The scale of the analyses is fixed by the size of the hexagonal cell, which is 16 km^2 for Svalbard and 4 km^2 for Isfjord. The maps show the differences in fast ice duration. The biggest differences are in the fjords of Spitsbergen, the greatest being in the northern ones. In the whole of this area, the duration has been reduced by 3-4 months. In the other fjords, such dramatic changes have occurred only locally; the reduction there has usually been from 1 to 3 months. In northern Svalbard, the duration of fast ice has decreased by 2 months; elsewhere, the changes are no greater than 1 month, and locally no more than 2 months. Figure 4b clearly shows the spatial variation revealed by the larger-scale analyses performed for Isfjord, while the temporal variation is from zero to 4-5 months. This implies that along the coast of this fjord there are some sites where the changes have been significant and others they have been negligible. The significant changes relate mainly to the fjord's branches, where the fast ice cover before 2000 was long-lasting.

https://doi.org/10.5194/tc-2021-21
Preprint. Discussion started: 12 March 2021

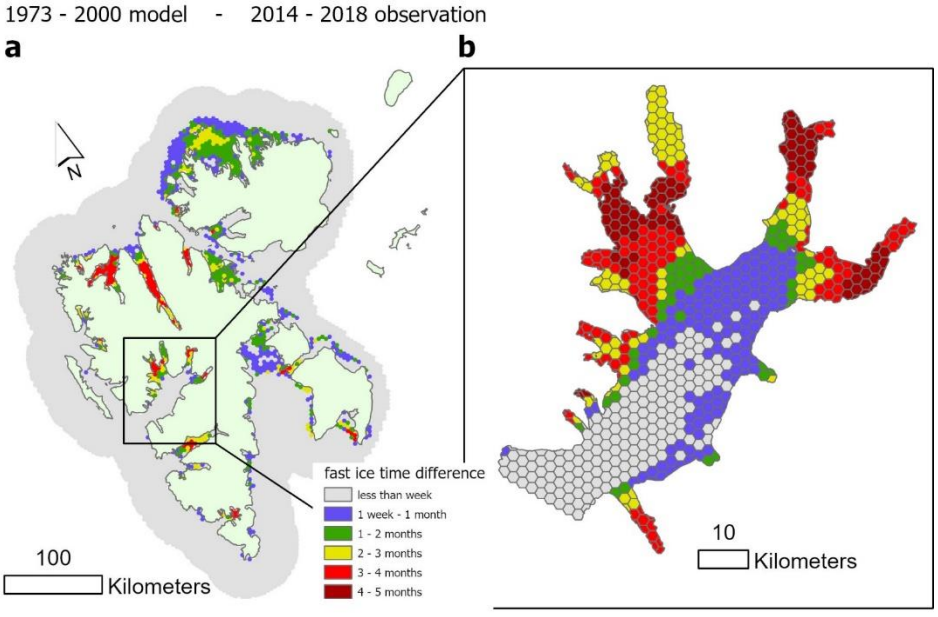

Figure 9: Mean distribution of the difference in fast ice extent in Svalbard (a) and Isfjord (b) during the ice seasons in 1973-2000 and 2014-2018. The maps show the difference between the durations of fast ice in both areas in both periods. Map (a) was produced using the 16 km^2 hexagon net, map (b) using the 4 km^2 hexagon net.

6. Conclusion

The summary of the project results in the shape of quantitative analyses is shown in Figure 10. All-time series of observations and modeling are presented. The lines show what is the duration of fast ice for a particular total ice cover area. The GeoRF model was created using observations from 2005-2018. For Isfjord about 50 additional observations for high FDD values were obtained from satellite images from the years 1973-1998. The replicated data generated under the model look similar to observed data (2005-2018, 2005-2018 model) with R^2 accuracy of 0.95. In this time fast ice cover was 8000 km^2 with at least 2 months duration and a bit above 5000 km^2 with at least 3 months duration. This model was also applied for years 2014-2019, when the rapid reduction in fast ice cover was observed to 6000 km^2 for two-month ice, to test its stability for other conditions (2014-2019, 2014-2019 model). The model performs well for longer fast ice cover but worse for ice cover with a shorter duration than 2 months. As well modeled as observational data show 2 months duration fast ice cover reduction by 25% and 50% reduction for ice with 3 months duration compare to 2005-2018. For the time before 2000 and predicted temperature rise of 2 and 4 ºC presented results are based only on the models. Assuming that the model error is proportional to the deviation of data used to prediction from the data for which it was originally created some measure of uncertainty may be deducted from Figure 10.

https://doi.org/10.5194/tc-2021-21
Preprint. Discussion started: 12 March 2021

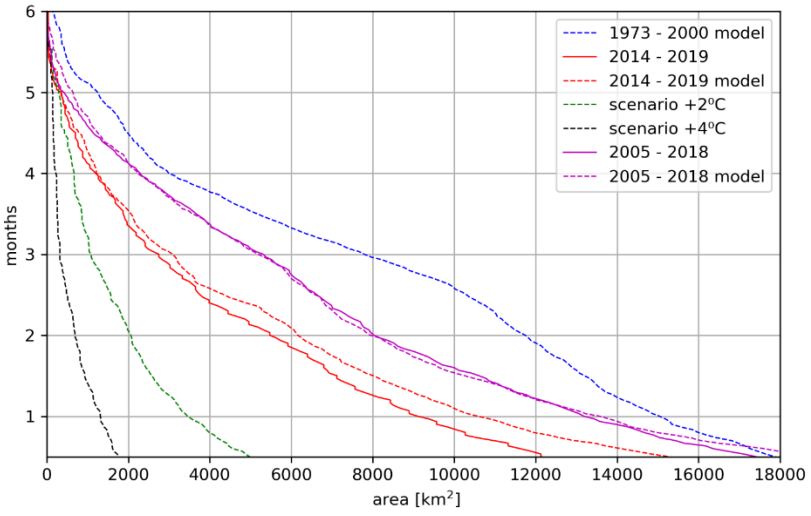

Figure 10: Months of fast ice with an extent at least than a specified area in km^2 obtained from observational data or geographically weighted random forest model. The solid lines represent results from observations and dashed lines results from the model. The model was created using the 2005 – 2018 data. Scenarios +2ºC and +4ºC are based on 2014 – 2019 data with the temperature increased by 2 or 4 degrees.

In years 1973-2000 at least 2 months lasting fast ice cover was 12000 ±250 km^2, and at least 3 months lasting 8000 ± 150 km^2. The reduction of fast ice cover in 2005-2018 comparing wits 1973-2000 is therefore 30-40%. The prediction of the consequences of further air temperature rice has only a speculative character. The temperature rise of 2 ºC will reduce the 2-month lasting cover to 2000 km^2 which is a 60% reduction comparing to the current situation. The maximum fast ice cover will be only 20% of these in the years 1973-2000. The rice of 4 ºC will reduce it further to 10%.

Author Contributions:

J.U. designed the study, analysed the data and was responsible for writing the manuscript. D.L. prepared the data for the project and edited the manuscript.

Competing interests:

The authors declare that they have no conflict of interest.

Acknowledgements

This work was carried out as part of the project ACCES "De-icing of Arctic Coasts: Critical or new opportunities for marine biodiversity and Ecosystem Services?" funded by the Belmont Forum, Call Title: Biodiversity2017 – Scenarios of Biodiversity and Ecosystem Services.

https://doi.org/10.5194/tc-2021-21
Preprint. Discussion started: 12 March 2021

References:

Breiman, L.: Random Forests, Mach. Learn., 45, 5-32, 2001

Georganos, S., Grippa, T., Niang Gadiaga, A., Linard, C., Lennert, M., Vanhuysse, S., Mboga, N., Wolff, E. and Kalogirou, S.: Geographical random forests: a spatial extension of the random forest algorithm to address spatial heterogeneity in remote sensing and population modelling, Geocarto Int., 0(0), 1–16, doi:10.1080/10106049.2019.1595177, 2019.

Gerland, S. and Hall, R.: Variability of fast-ice thickness in Spitsbergen fjords, Ann. Glaciol., 44(9296), 231–239, doi:10.3189/172756406781811367, 2006.

Gerland, S. and Renner, A. H. H.: Sea-ice mass-balance monitoring in an Arctic fjord, Ann. Glaciol., 46(9296), 435–442, doi:10.3189/172756407782871215, 2007.

Gerland, S., Renner, A. H. H., Godtliebsen, F., Divine, D. and Løyning, T. B.: Decrease of sea ice thickness at Hopen, Barents Sea, during 1966-2007, Geophys. Res. Lett., 35(6), 1–5, doi:10.1029/2007GL032716, 2008.

Hanssen-Bauer, I., Førland, E. J., Hisdal, H., Mayer, S., Sandø, A. B., Sorteberg, A., Adakudlu, M., Andresen, J., Bakke, J., Beldring, S., Benestad, R., Bilt, W., Bogen, J., Borstad, C., Breili, K., Breivik, Ø., Børsheim, K. Y., Christiansen, H. H., Dobler, A., Engeset, R., Frauenfelder, R., Gerland, S., Gjelten, H. M., Gundersen, J., Isaksen, K., Jaedicke, C., Kierulf, H., Kohler, J., Li, H., Lutz, J., Melvold, K., Mezghani, A., Nilsen, F., Nilsen, I. B., Nilsen, J. E. Ø., Pavlova, O., Ravndal, O., Risebrobakken, B., Saloranta, T., Sandven, S., Schuler, T. V, Simpson, M. J. R., Skogen, M., Smedsrud, L. H., Sund, M., Vikhamar-Schuler, D., Westermann, S. and Wong, W. K.: Climate in Svalbard 2100, , (1) [online] Available from: http://www.miljodirektoratet.no/M1242, 2019.

Isaksen, K., Nordli Ø., Førland E. J., Łupikasza E., Eastwood S., N. T.: Recent warming on Spitsbergen—Influenceof atmospheric circulation and sea ice cover, J. Geophys. Res. Atmos., 121, 11,913-11,931, doi:10.1002/2016JD025606, 2016.

Krafft, B. A., Kovacs, K. M., Andersen, M., Aars, J., Lydersen, C., Ergon, T. and Haug, T.: Abundance of ringed seals (Pusa hispida) in the fjords of Spitsbergen, Svalbard, during the peak molting period, Mar. Mammal Sci., 22(2), 394–412, doi:10.1111/j.1748-7692.2006.00035.x, 2006.

Lepparanta, M.: A review of analytical models of sea-ice growth, Atmos. - Ocean, 31(1), 123–138, doi:10.1080/07055900.1993.9649465, 1993.

Lutz, S. R., Krieg, R., Müller, C., Zink, M., Knöller, K., Samaniego, L. and Merz, R.: Spatial Patterns of Water Age: Using Young Water Fractions to Improve the Characterization of Transit Times in Contrasting Catchments, Water Resour. Res.,

54(7), 4767–4784, doi:10.1029/2017WR022216, 2018.

Menne, M.J., I. Durre, B. Korzeniewski, S. McNeal, K. Thomas, X. Yin, S. A. and R. Ray, R.S. Vose, B.E.Gleason, Houston, T. G.: Global Historical Climatology Network - Daily (GHCN-Daily), Version 3., 2012.

Muckenhuber, S., Nilsen, F., Korosov, A. and Sandven, S.: Sea ice cover in Isfjorden and Hornsund, Svalbard (2000-2014) from remote sensing data, Cryosphere, 10(1), 149–158, doi:10.5194/tc-10-149-2016, 2016.

Mutanga, O., Adam, E. and Cho, M. A.: High density biomass estimation for wetland vegetation using WorldView-2 imagery and random forest regression algorithm, Int. J. Appl. Earth Obs. Geoinf., 18, 399–406, doi:10.1016/j.jag.2012.03.012, 2012.

Nordli, Ø., Przybylak, R., Ogilvie, A. E. J. and Isaksen, K.: Long-term temperature trends and variability on spitsbergen: The extended svalbard airport temperature series, 1898-2012, Polar Res., 33(1 SUPPL), doi:10.3402/polar.v33.21349, 2014.

Pavlov, A.K.: The Underwater Light Climate in Kongsfjorden and Its Ecological Implications, in The Ecosystem of Kongsfjorden, Svalbard, edited by H. Haakon and C. Wiencke, pp. 137–170, Springer., 2019.

Pedregosa, F.,Varoquaux, G., Gramfort, A., Michel, V., Thirion,B., Grisel, O., Blondel, M., Prettenhofer, P., Weiss, R., Doubourg, V., Vaderplas, J., Passos, A., Cournapeau, D., Brucher, M., Perrot, M., Duchesnay, E.: Scikit-learn: Machine Learning in Python, J. Mach. Learn. Res., 12, 2825–2830, 2011.

Rodriguez-Galiano, V., Mendes, M. P., Garcia-Soldado, M. J., Chica-Olmo, M. and Ribeiro, L.: Predictive modeling of groundwater nitrate pollution using Random Forest and multisource variables related to intrinsic and specific vulnerability: A case study in an agricultural setting (Southern Spain), Sci. Total Environ., 476–477, 189–206, doi:10.1016/j.scitotenv.2014.01.001, 2014.

Rodriguez-Galiano, V., Sanchez-Castillo, M., Chica-Olmo, M. and Chica-Rivas, M.: Machine learning predictive models for mineral prospectivity: An evaluation of neural networks, random forest, regression trees and support vector machines, Ore Geol. Rev., 71, 804–818, doi:10.1016/j.oregeorev.2015.01.001, 2015.

Smith, T. G. and Lydersen, C.: Availability of suitable land-fast ice and predation as factors limiting ringed seal populations, Phoca hispida, in Svalbard, Polar Res., 10(2), 585–594, doi:10.1111/j.1751-8369.1991.tb00676.x, 1991.

Wang, C., Shi, L., Gerland, S., Granskog, M. A., Renner, A. H. H., Li, Z., Hansen, E. and Martma, T.: Spring sea-ice evolution in Rijpfjorden (80° N), Svalbard, from in situ measurements and ice mass-balance buoy (IMB) data, Ann. Glaciol., 54(62), 253–260, doi:10.3189/2013AoG62A135, 2013.

https://doi.org/10.5194/tc-2021-21
Preprint. Discussion started: 12 March 2021

Zakhvatkina, N., Smirnov, V. and Bychkova, I.: Satellite SAR data-based sea ice classification: An overview, Geosci., 9(4), 3–5, doi:10.3390/geosciences9040152, 2019.

Zhuravskiy, D., Ivanov, B. and Pavlov, A.: Ice conditions at Gronfjorden bay, Svalbard, from 1974 to 2008, Polar Geogr., 35(2), 169–176, doi:10.1080/1088937X.2012.662535, 2012.